

## EXPERIMENTAL MEASUREMENT OF TWO-PHASE RELATIVE PERMEABILITY IN VERTICAL FRACTURES

Nick Speyer, Kewen Li, Roland Horne

Stanford University  
067 Green Earth Science Bldg.  
Stanford, CA, 94305, USA

e-mail: [nspeyer@stanford.edu](mailto:nspeyer@stanford.edu), [kewenli@stanford.edu](mailto:kewenli@stanford.edu), [horne@stanford.edu](mailto:horne@stanford.edu)

### **ABSTRACT**

Relative permeability characteristics in porous media have been extensively studied and are reasonably well understood. However there have been comparatively few studies of relative permeability in fractures. Given that geothermal reservoir permeabilities are almost always dominated by fractures, understanding of fracture relative permeabilities is essential for accurate geothermal reservoir simulation. Nitrogen-water relative permeabilities were measured in a manufactured vertical fracture and two-phase flow structures were observed and correlated with different flow regimes.

### **INTRODUCTION**

Generalized Darcy equations can be used to describe flow rates in fractures.

$$q_l = k_{abs} A k_{rl} (p_i - p_o) / \mu_l L \quad (1)$$

$$q_g = k_{abs} A k_{rg} (p_i - p_o) / \mu_g L \quad (2)$$

Where  $l$  and  $g$  indicate liquid and gas respectively,  $k_{abs}$  is the absolute permeability of the fracture,  $p_i$  and  $p_o$  are the respective pressures at the inlet and outlet of the fracture,  $\mu$  is the viscosity,  $L$  is the length of the fracture, and  $k_{rl}$  and  $k_{rg}$  are the liquid and gas relative permeabilities, respectively. In order to consider the compressibility of the gas phase, Equation (2) can be written as:

$$u_g = \frac{k_{abs} k_{rg} (p_i^2 - p_o^2)}{2 \mu_g p_o L} \quad (3)$$

The theoretical absolute permeability of a fracture with aperture  $h$  can be derived to be:

$$k_{abs} = \frac{h^2}{12} \quad (4)$$

Relative permeability describes the permeability of one phase in the presence of another.

$$k_{rw} = \frac{k_w}{k_{abs}} \quad (5)$$

$$k_{rg} = \frac{k_g}{k_{abs}} \quad (6)$$

In the absence of any phase interference, the sum of  $k_{rg}$  and  $k_{rw}$  will be 1. This is rarely the case in real rocks. The interference effect can be quantified by the difference between 1 and the sum of the two relative permeabilities. In general, the lower the sum of the two relative permeabilities, the greater the phase interference.

Accurate reservoir simulation cannot take place without some knowledge of the relative permeability characteristics. The relative permeabilities are commonly expressed as functions of the saturations, end-point values and irreducible saturations of the different fluids in three different models. The simplest model is the X-Model, which assumes no interference between phases, and pure laminar flow (i.e. gas and water flowing parallel next to each other):

$$k_{rw} = S_w \quad (7)$$

$$k_{rg} = S_g \quad (8)$$

With  $S_w$  and  $S_g$  being the mobile water and gas saturations respectively. This model has the sum of  $k_{rg}$  and  $k_{rw}$  equal to 1. In real fractures, interactions between fluids and between fluids and the fracture surface can have an effect on the relative permeabilities, so a more comprehensive model may be more appropriate.

In earlier experiments on horizontal fractures, relative permeabilities have been found to be very similar to the Corey (1954) curves used for relative permeability in homogeneously porous media (Diomampo, 2001; Chen, 2005):

$$k_{rl} = (S^*)^4 \quad (9)$$

$$k_{rg} = (1 - S^*)^2 (1 - S^{*2}) \quad (10)$$

With  $S^*$  defined as:

$$S^* = \frac{(S_l - S_{rl})}{(1 - S_{rl} - S_{rg})} \quad (11)$$

With  $S_{rl}$  and  $S_{rg}$  being the irreducible residual saturations of liquid and gas respectively. A third model treats the fracture like a system of pipes, including the viscosities of the two fluids and also incorporates wettability effects. This model is known as the viscous coupling model (Fourar and Lenormand, 1998):

$$k_{rl} = \frac{S_l^2}{2} (3 - S_l) \quad (12)$$

$$k_{rg} = (1 - S_l)^3 + \frac{3}{2} \mu_r S_l (1 - S_l) (2 - S_l) \quad (13)$$

With  $\mu_r = \mu_g/\mu_l$ . With a liquid and a gas,  $\mu_g \ll \mu_l$ , so  $\mu_r$  is very close to zero which means that the second term of Equation (13) can be ignored.

### **Previous Work**

There have been several experimental studies that have investigated fracture relative permeabilities (Fourar et al., 1993; Persoff and Pruess, 1995; Diomampo, 2001; Chen 2005).

Fourar et al. (1993) measured relative permeability using a synthetic fracture consisting of two horizontal glass plates of varying textures. Different textures were created by gluing small glass beads to the surfaces. They injected water and gas at set rates while measuring pressure and saturation and described the flow according to three models: relative permeabilities, pipe flow, and as a homogeneous flow in rough tube. High phase interference between gas and water was observed to the degree that the sum of the two relative permeabilities was never equal to 1. It was also found that the relative permeabilities were not strict functions of  $S_w$ , but also depended on the liquid velocity in the fracture. Flow structures were observed and correlated with different flow rates and ratios. Persoff and Pruess (1995) created a copy of a

natural fracture by creating a mold of each side of a natural fracture and creating epoxy replicas from those molds. Relative permeability measurements were made and significant phase interference was again detected. Although the results did not match well with any of the major relative permeability models, it was concluded that treating fractures as very heterogeneous two-dimensional porous media is appropriate.

Diomampo (2001) measured nitrogen-water relative permeabilities in a horizontal fracture between glass and aluminum. High phase interference was observed as well as continuous instability of flow channels. A good match with the Corey-type relative permeability curves was found. Chen (2005) conducted nitrogen-water and steam-water relative permeability experiments on the same apparatus and correlated different flow regimes to flow structures quantitatively. Steam relative permeabilities were seen to be greater than comparable nitrogen relative permeabilities due to phase transformation effects. The goal of the present work has been to build on the work of Chen and Diomampo in horizontal fractures, and determine the effect of fracture orientation by measuring relative permeabilities in a vertical fracture.

### **METHODS**

In this study, gas-water flow experiments were conducted at 24°C. The fluids consist of pure nitrogen and deionized water. The water is exposed to the air before injection and the nitrogen is bubbled through water so as to achieve solubility equilibrium and thereby minimize evaporation and condensation within the apparatus. The water injection is controlled by a Dynamax SD-600 solvent delivery system. Gas injection is controlled through a flow regulator (Brooks Instrument, Flow Controller Model 0151E), which is connected to a gas meter (Brooks Instrument, Flow Meter model 5850E, max. rate: 200 ml/min). All measurements are electronic and digitized by using high-speed data acquisition system (DAQ; National Instrument, SCXI-1000 with PCI 6023E A/D board) and digital video recording system (Sony Digital-8 560X with Pinnacle Studio DV IEEE 1394 image capture card). The whole experimental system is illustrated in Figure 1, which shows the fluid supply, the fracture apparatus, data acquisition system, and digital image recording.

### **Fracture Apparatus**

The fracture used for the experimental measurements was the space between a plate of glass and a flat aluminum surface. It is necessary to have one wall of the fracture be transparent in order to measure  $S_w$  visually as described later. The glass surface can be changed to experiment with different textures. In this case a piece of homogeneously rough (HR) glass was

used.

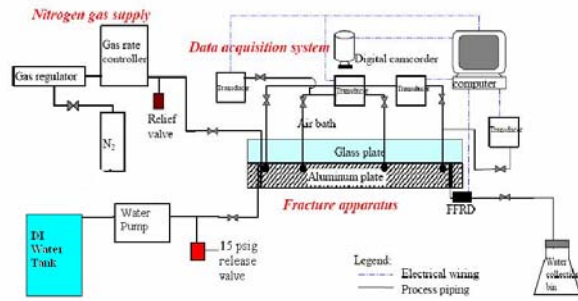


Figure 1. Schematic of experimental apparatus. (Chen, 2005).

The water and gas are delivered at individually controlled rates to the fracture apparatus. The two plates are held together by an aluminum frame which is mounted vertically. The fracture surface measures 30.48cm x 10.16cm. The fracture aperture is created by a layer of gasket sealant around the edge of the glass. There are four pressure ports drilled in the aluminum plate for pressure transducer access. The incoming gas and water are dispersed evenly at the inlet through 123 small alternating channels and are drained through a single outlet. The fracture apparatus is kept in a temperature controlled air-bath that is kept at 24°C for the air-water experiments. (Figure 2)

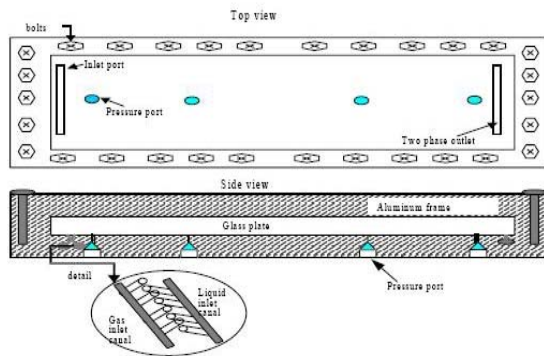


Figure 2. Diagram of fracture apparatus. (Chen, 2005).

Low-range differential transducers were used to measure the pressure difference through the fracture, as well as the intermediate pressure and the two-phase outlet pressure. Two liquid differential transducers (Validyne Transducer, model DP-15, range 0-2 psig) are attached to four pressure ports inside the fracture to measure the pressure difference through the fracture. Another transducer (Validyne Transducer, model DP-15, range 0-5 psig) is attached to the upstream end of the middle differential transducer. The fourth transducer (Validyne Transducer, model DP-15, range 0-5 psig) is attached

to the two-phase outlet of the fracture apparatus. These transducers send electrical signals to the data acquisition system, which is monitored using the LabView® programmable virtual instrument software. The complete measurement configuration in the fracture apparatus is shown in Figure 1.

### FFRD

Aside from the known input rates, to obtain the instantaneous flow rates, a fractional flow ratio detector (FFRD) is used as shown in Figure 1. The FFRD is used to measure the outlet gas and water fractional flows,  $f_g$  and  $f_w$ .

$$f_g = \frac{q_{out,g}}{q_{out,t}} \quad \text{with} \quad q_{out,t} = q_{out,w} + q_{out,g} \quad (14,15)$$

$$f_w = \frac{q_{out,w}}{q_{out,t}}$$

where  $q_{out,g}$  is the outlet gas flow rate,  $q_{out,w}$  is the outlet water flow rate, and  $q_{out,t}$  is the outlet total flow rate. The principle of the FFRD is that different phases will have different refractive indices. A phototransistor (NTE 3038, NPN-Si, Visible) is installed inside the FFRD with a small LED bulb and connected. The phototransistor transmits different voltages when sensing different strengths of light. The water phase produces a higher voltage than the gas when flowing through the FFRD. The gas and water phase flow ratios are obtained by determining the ratio of the number of gas and water signals. Once  $f_g$  and  $f_w$  are obtained at steady-state condition, it is easy to calculate  $q_{out,g}$  by assuming that water flow rate remains constant from inlet to outlet of the fracture. This assumption can hold if the wetting phase (water) flows in a continuous channel, and the water viscosity is much larger than the nonwetting phase.

The FFRD was not used in the nitrogen-water experiments because the absolute flow rates are known exactly. In the steam-water experiments, the flow of both phases is unknown, and thus it is necessary to infer the two flow rates using the FFRD.

### Saturation Measurements

Continuous saturation measurements are necessary for the calculation of relative permeability functions. During the experiment, the flow is recorded through the glass plate using a digital camcorder at 29.97 frames/second. This video is then turned to still images using a Matlab® program that captures frames with any assigned frequency (in this case 5 per second). The images are then cropped and turned into binary images which can then be used for a saturation calculation (black pixels are water, white pixels are gas). For the rough-walled fractures, there

are many shadow effects and uneven distributions of light, so obtaining accurate binary images is not straightforward. The image is divided up into 16 sectors. Each sector is then assigned a threshold brightness which the program uses to decide whether a given pixel is white or black. The threshold for each sector is assigned by trial and error. This is a very effective, although time consuming, technique. The end result is an array of time-stamped saturation measurements that can be correlated with time-stamped pressure and FFRD measurements. A sample result is shown in Figure 3.

### Experimental Procedure

To calculate  $k_{rw}$  experimentally according to equation (1) one needs to know  $k, A, \Delta P, L, \mu_w$  and  $\mu_g$ . To calculate  $k_{rg}$  according to Equation (3), one also needs explicit inlet and outlet pressures. The fracture length and viscosities are known, and the necessary pressures are measured, but the absolute permeability ( $k$ ) and cross-sectional area ( $A$ ) values are not known for the fracture. It is impossible to measure  $k$  or  $A$  explicitly using Darcy's law without knowing one of them to begin with. For the smooth-walled fracture,  $A$  can be calculated because the width of the fracture is relatively well constrained, but with the rough-walled fractures, determination of  $A$  is not so straightforward. Although the two variables cannot be measured explicitly, their product can be measured using Darcy's law. Before each set of relative permeability measurements was made, the fracture was fully saturated with water flowing at different rates while the pressure gradient across the fracture and the pressure in the middle of the fracture were monitored. The result was an array of  $kA$  values corresponding to different fracture pressures. This function was used for the  $kA$  values in the relative permeability calculations. The  $kA$  function

was calculated every morning that an experiment took place. An example can be seen in Figure 4.

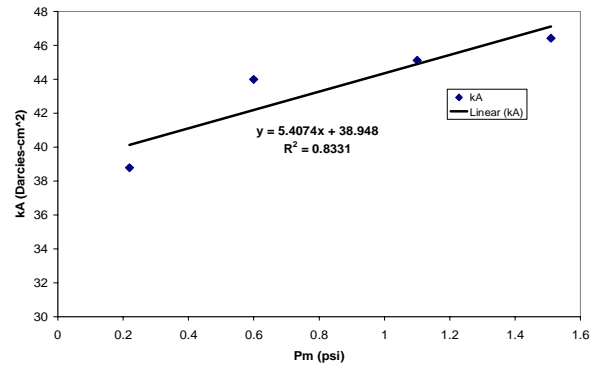


Figure 4. Measured  $kA$  values plotted against fracture pressure and fitted with a linear function.

To measure the relative permeabilities, the fracture was initially saturated with water. Gas was then injected into the fracture at a very low rate (2.7  $\text{cm}^3/\text{min}$  was the lowest rate used) with water injected at a high rate (10  $\text{cm}^3/\text{min}$  was the highest used) and the system was allowed to reach a steady state, or as steady as could be achieved given the sometimes dynamic nature of the flow structures. The system was run as such for roughly two minutes while being videotaped and with DAQ system running. Then the gas rate was increased and the system state was recorded again. Once the maximum gas rate was reached, the fracture was resaturated with water and the procedure was repeated using a lower water flow rate. Gas rates varied from 2.7  $\text{cm}^3/\text{min}$  to 200  $\text{cm}^3/\text{min}$  and water rates varied from 10  $\text{cm}^3/\text{min}$  to .2  $\text{cm}^3/\text{min}$ . The data from each run was tabulated using Microsoft Excel.



Figure 3. Sample images showing corresponding color and binary images. The light phase is water and the dark phase is gas in the color image. In the binary image, the black is water and the white is gas.

## RESULTS

Using the homogeneously rough glass, nitrogen-water relative permeability measurements were made at 24°C. Due to the vertical orientation of the fracture and the lack of a distributed drainage system, there were significant end effects visible in the flow structures. Only the middle third of the fracture was observed for flow structure and saturation measurements. These measurements were done twice with similar results (Figure 6). Two important differences were observed in the nature of the two-phase flow.  $S_{wr}$  was 0.64 compared with 0.25 which had been measured in the exact same apparatus oriented horizontally (Chen 2005). (Figure 5) Also, the flow structures observed were relatively stable except at very high gas flow rates, with the gas preferentially (but not exclusively) flowing along the top edge of the fracture.

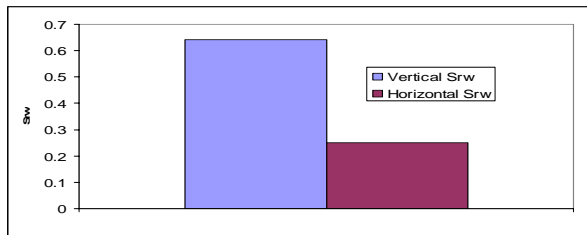


Figure 5. Comparison of  $S_{wr}$  for horizontal and vertical fractures.

In these experiments, horizontal flow through vertical fractures was simulated. Layered flow was anticipated, with the gas flowing over the water with very little phase interference, thus leading to an X-curve type relative permeability regime. This was a partially accurate hypothesis. Layered flow was observed with very low gas flow rates. Once  $q_g$  increased past  $\sim 20 \text{ cm}^3/\text{min}$ , the gas flowed through

stable subhorizontal tortuous channels near the top of the fracture in addition to flowing along the top edge. As  $q_g$  increased further, the downward infiltration of gas channels continued until two-phase flow was occurring in the top two-thirds of the fracture (Figure 3). The bottom half of the fracture was not infiltrated by gas at all until  $q_g=200 \text{ cm}^3/\text{min}$ , at which point a stable gas channel was created across the bottom edge of the fracture. The channels were very stable with low flow rates, but became more dynamic and even turbulent, exhibiting slug flow with higher  $q_g/q_w$  coupled with high overall flow rates.

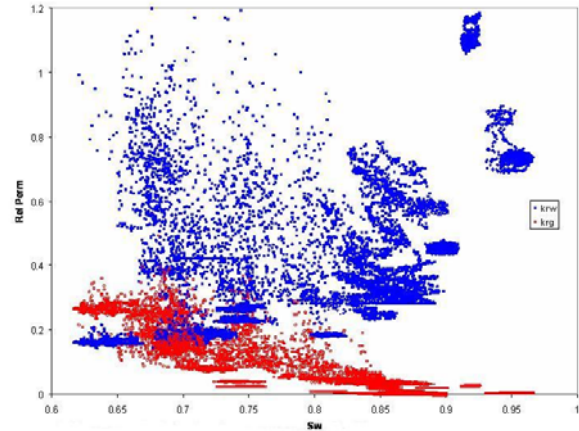


Figure 7. Raw relative permeability data.

## DISCUSSION

Of the three relative permeability models discussed previously, none describe the measured relative permeabilities very well. At high water saturations, the Corey model looks to be a reasonable approximation at some saturations, but there seems to be too much variability. The X-curve which could have been expected is clearly not a good approximation of vertical fracture relative

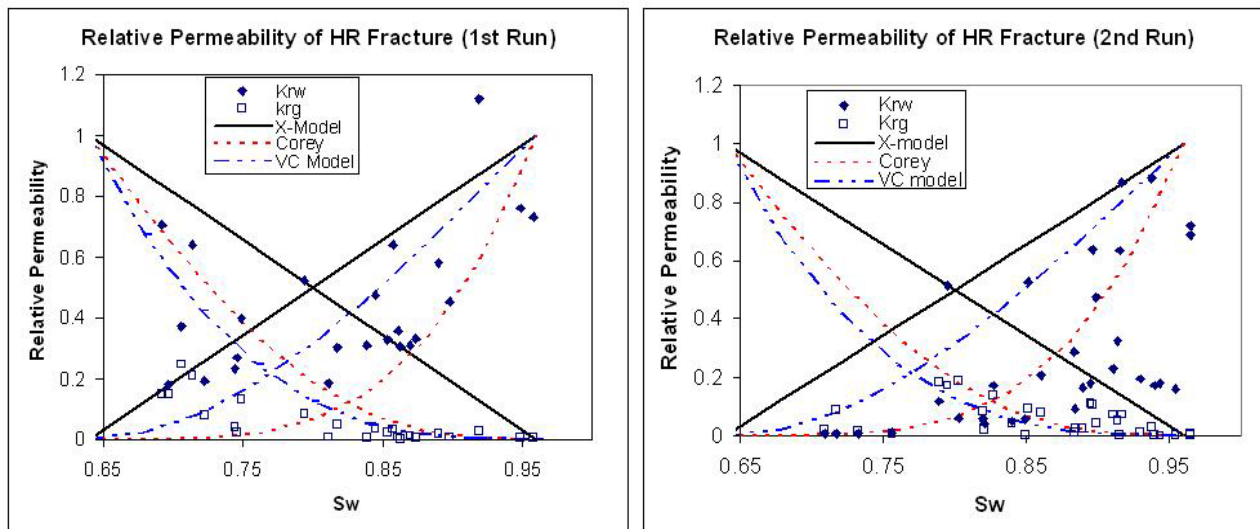


Figure 6. Averaged measured relative permeabilities compared with the X-model, Corey model, and viscous-coupling model. The plotted data are the average  $k_{rw}$  and  $k_{rg}$  values for each individual flow regime (e.g.  $q_w=10 \text{ cm}^3/\text{min}$ ;  $q_g=5 \text{ cm}^3/\text{min}$ ).

permeability and neither is the viscous coupling model. The viscous coupling model approximates pipe flow, which has no residual saturations. Given the magnitude of the residual saturations measured in this study, it is not surprising that the viscous coupling model does not do a good job of predicting the experimental results. Given the variability of the measured data, it may be the case that no single existing model can accurately predict relative two-phase relative permeability in vertical fractures.

There are clearly some problems with the data that will require further tuning of the experimental technique. Some water relative permeabilities were above 1, which should not be possible. Also, the data are very noisy, much more so than the data of Chen (2005) who used the exact same apparatus oriented horizontally.

Three problems are apparent with the apparatus, first is the outlet at the end of the fracture, which is a single hole in the middle of a linear gap that runs the entire width of the fracture. This was of no concern when the fracture was oriented horizontally, because there was no gravitational segregation of the two phases. However, with the vertical fracture, the outlet is well below the top edge of the fracture which is where the gas flows preferentially. This causes the gas flow path to deviate downwards at the end of the fracture. Either a longer fracture, or a more distributed exhaust system would remedy this problem. The second problem is that the fracture measures only 10.16cm in the vertical direction. The behavior observed in this study may not necessarily scale to larger fractures. The third problem is that the flow rates measured are very limited in scale compared with the range of flow rates that have been observed in geothermal reservoirs.

### **Future Work**

The next step in this research will be to measure steam-water relative permeabilities and to experiment with different glass textures to represent different fracture surface roughness.

### **REFERENCES**

1. Chen, A.: "Liquid-Gas Relative Permeabilities in Fractures: Effects of Flow Structures, Phase Transformation and Surface Roughness". PhD Thesis, Stanford University, Stanford, CA (2005).
2. Corey, A.T.: "The interrelation between Gas and Oil Relative Permeabilities". *Prod. Mon.* (1954), Vol. 19, pp. 38-41.
3. Diomampo, G.P.: "Relative Permeability through Fractures". MS Thesis. Stanford University, Stanford, California (2001).
4. Fourar, M., Bories, S., Lenormand, R., Persoff, P.: "Two-phase flow in smooth and rough fractures: Measurement and correlation by porous-medium and pipe-flow models" *Water Resources Research* Vol. 29, No. 11, November 1993, pp. 3699-3708.
5. Fourar, M., Lenormand, R.: "A Viscous Coupling Model for Relative Permeabilities in Fractures" SPE 49006, paper presented at the SPE Annual Technical Conference and Exhibition, New Orleans, LA, USA. 1998.
6. Persoff, P. and Pruess, K.: "Two-phase flow visualization and relative permeability measurement in natural rough-walled rock fractures", *Water Resources Research* Vol. 31, No. 5, May 1995, pp. 1175-1186.